


Article

# Formation of Palygorskite Clay from Treated Diatomite and its Application for the Removal of Heavy Metals from Aqueous Solution

Houwaida Nefzi <sup>1,2,3</sup>, Manef Abderrabba <sup>1</sup>, Sameh Ayadi <sup>1</sup> and Jalel Labidi <sup>3,\*</sup> 

<sup>1</sup> Laboratory of Materials, Molecules and Applications, IPEST, Preparatory Institute of Scientific and Technical Studies of Tunis, University of Carthage, SidiBou Said road, B.P. 512070, La Marsa 1054, Tunisia; houayda.89@gmail.com (H.N.); abderrabbamanef@gmail.com (M.A.); sameh.ayadi@instm.rnrt.tn (S.A.)

<sup>2</sup> Chemistry Department, Faculty of Sciences of Tunis, El Manar University, B.P. 248, El Manar II, Tunis 2092, Tunisia

<sup>3</sup> Biorefinery Processes Research Group, Department of Chemical and Environmental Engineering, University of the Basque Country (UPV/EHU), Plaza. Europa1, 20018 Donostia-San Sebastian, Spain

\* Correspondence: Jalel.Labidi@ehu.es; Tel.: +34-943-017-178

Received: 13 August 2018; Accepted: 12 September 2018; Published: 15 September 2018



**Abstract:** Environmental contamination by toxic heavy metals is a serious worldwide phenomenon. Thus, their removal is a crucial issue. In this study, we found an efficient adsorbent to remove  $\text{Cu}^{2+}$  and  $\text{Ni}^{2+}$  from aqueous solution using two materials. Chemical modification was used to obtain palygorskite clay from diatomite. The adsorbents were characterized using X-ray fluorescence, Fourier transform infrared spectroscopy and X-ray diffraction. The effects of contact time, initial concentration, temperature and pH on the adsorption process were investigated. Our results showed that the (%) of maximum adsorption capacity of diatomite was 78.44% for  $\text{Cu}^{2+}$  at pH 4 and 77.3% for  $\text{Ni}^{2+}$  at pH 7, while the (%) of the maximum adsorption on palygorskite reached 91% for  $\text{Cu}^{2+}$  and 87.05% for  $\text{Ni}^{2+}$ , in the same condition. The results indicate that the pseudo-second-order model can describe the adsorption process. Furthermore, the adsorption isotherms could be adopted by the Langmuir and the Freundlich models with good correlation coefficient ( $R^2$ ). Thus, our results showed that palygorskite prepared from Tunisian diatomite is a good adsorbent for the removal of heavy metals from water.

**Keywords:** palygorskite clay; diatomaceous earth; heavy metals; adsorption capacity

## 1. Introduction

Heavy metal ions play a very important role in certain industries due to their technological importance. However, they pose serious dangerous effects because they are persisting in the environment. In addition, metal ions have a chronic toxicity, persistency and accumulation tendency in body tissues. For example, copper is known as the highest mammalian toxic specie; its inhalation is linked with an augmentation in lung cancer and its accumulation in the vital organs causes many diseases and disorders [1]. It is widely used in ornamental ponds and in water supply reservoirs. Nickel is recognized as the most recalcitrant pollutant. It is not biodegradable and can cause dermatitis, allergic sensitization, respiratory distress and dizziness. It is extensively used in electroplating, zinc base casting, battery industries and silver refineries. Thus, the removal of  $\text{Cu}^{2+}$  and  $\text{Ni}^{2+}$  is considered of high importance. Traditional methods were applied for heavy metals elimination such as ion exchange, chemical precipitation, membrane filtration, biological treatment and adsorption [2,3]. Among all these technologies, adsorption is the most useful method due to its efficiency and lower cost. For this purpose, many researchers used various kinds of low-cost and natural adsorbents, such as coconut coir

pith, sludge ash, diatomite and different type of minerals clays, such as palygorskite, kaolin, sepiolite, montmorillonite and so forth.

Palygorskite, known also as attapulgite, is a kind of a mineral clay; it is crystalline hydrated magnesium silicate consisting of a type of 2:1 layer phyllosilicate (tetrahedral: octahedral) [4,5]. Palygorskite contains mainly  $Mg^{2+}$  and other cations such as  $Fe^{3+}$  and  $Al^{3+}$  with significant quantities [6]. Bradley reported the ideal structure of palygorskite  $\{(Mg,Al)_4Si_8(O,OH,H_2O)_{24}\cdot nH_2O\}$  for the first time in 1940 [7]. Furthermore, this kind of clay has numerous advantages: a high adsorption capacity, fibrous morphology, porous structure, high surface area, moderate cation exchange, excellent salt residence and charge in the lattice [8]. Due to its special properties, palygorskite has gained attention from the chemical industry. It can be used in ion exchange, catalysis and water softening. In addition, the literature provides various works for the removal of heavy metals using palygorskite in its natural and modified state. Due to these abundant uses, the consumption of palygorskite increases rapidly and calls for further work seeking cheaper and natural materials for their synthesis. Palygorskite may be obtained from other clays. Despite the various applications of palygorskite, very few reports have shown its preparation from other mineral clay, so there are no references indicating its formation or synthesis from natural rock, such as diatomaceous earth. Previous work reports the formation of other kinds of clay from palygorskite or diatomite, such as the formation of kaolinite from palygorskite and sepiolite [9]. In addition, A. Chaisena performed the synthesis of sodium zeolite from natural and modified diatomite [10].

Diatomaceous earth or diatomite ( $SiO_2 \cdot nH_2O$ ) is a sedimentary rock with a porous structure, low conductivity coefficient and low density. It consists essentially of high quantities of silicon dioxide  $SiO_2$  and low quantities of  $Al_2O_3$  and  $Fe_2O_3$  according to the clay impurities such as palygorskite and montmorillonite [11]. Additionally, the reactivity of diatomite is linked to the reactivity of the hydroxyl groups and the acid sites on the surface of the amorphous silica. Due to its specific characteristics, diatomite has attracted extensive research attention as an adsorbent for its natural and modified structure for the removal of heavy metals.

In order to meet the big demand of palygorskite, our study focuses on the synthesis of palygorskite clay from Tunisian diatomite as cheap raw materials. To confirm its efficiency, the prepared clay was used to remove  $Cu^{2+}$  and  $Ni^{2+}$  from aqueous solution and compared its adsorption capacity with natural diatomite powder. All adsorbents were characterized via XRF, XRD and FTIR. Thereafter, the effect of certain factors (contact time, initial concentration, temperature and pH) on the adsorption process were evaluated. In addition, the use of pseudo-first- and pseudo-second-order models for analyzing the adsorption systems was investigated and the applicability of two known isotherm models (Langmuir and Freundlich) was studied. Lastly, the thermodynamics parameters were calculated at different temperatures for  $Cu^{2+}$  and  $Ni^{2+}$  adsorption on diatomite and palygorskite.

## 2. Materials and Methods

### 2.1. Materials

The raw diatomite was obtained in Gafsa, Tunisia. Palygorskite was prepared from diatomite using hydrochloric acid HCl (Panreac, 37%), sodium hydroxide NaOH (Sigma Aldrich, USA  $\geq 98\%$ ), iron (III) chloride 6-hydrate  $FeCl_3 \cdot 6H_2O$  (Panreac, %) and magnesium chloride hexahydrate  $Cl_2Mg \cdot 6H_2O$  (Fluka, %). The chemicals tested were copper chloride  $CuCl_2$  (Merck, 98%) and ammonium nickel (II) sulfate hexahydrate  $(NH_4)_2Ni(SO_4)_2 \cdot 6H_2O$  (Sigma Aldrich, USA  $\geq 98$ ). All the chemical components were used without any purification.

### 2.2. Preparation of Palygorskite

The raw diatomite was completely crushed with hammers to obtain a powder sample. Then, an acid solution was used (HCl 2M) to remove fine and other adhered impurities. Specifically, the crushed powder was mixed with HCl at a solid g/mL ratio of 10% at room temperature for 3 h.

Finally, the resulting material was filtered and rinsed with HCl and distilled water several times and then dried into a vacuum oven at 100 °C for 24 h.

The preparation of palygorskite from treated diatomite was carried out using the procedure reported in literature [12–15]: 3 g of treated diatomaceous earth was mixed with 5 mL of 1 M of MgCl<sub>2</sub> under ultrasonic vibration for 30 min. Then, 1 M of FeCl<sub>3</sub> was added to the mixture. After 1 h, 50 mL of 2 M NaOH was added slowly under continuous agitation for 24 h. Lastly, the mixture was filtered and washed with distilled water several times to remove Cl<sup>−</sup>. The final sample was oven dried at 100 °C for 24 h.

### 2.3. Kinetics Batch Experiments

The experiments were conducted in 250 mL Erlenmeyer flasks containing 0.5 g of adsorbent and 50 mL of copper(II) ornickel(II) solutions, varying the concentrations from 40 to 100 mg/L. The flasks were agitated on a shaker at 300 rpm and room temperature. Samples were taken at predetermined time intervals (0, 5, 10, 15, 20, 30, 40, 60, 90 and 180 min) to determine the residual metal ion concentrations in the solution. The pH solution was adjusted using NaOH (0.1 M) and HCl (0.1 M). The solution was filtered through a 0.22 μm membrane filter. The concentration of heavy metals ions remaining in each solution was determined by spectrophotometry using the following calorimetric method: 10% of ethylenediaminetetraacetic acid (EDTA) was added to the Cu<sup>2+</sup> suspension to form a blue specific complex [16,17] and 1% of dimethylglyoxime (DMG) was added for the Ni<sup>2+</sup> solution; this reagent forms a red complex [18,19]. The absorbance was measured after 30 min at 750 nm and 465 nm for Cu<sup>2+</sup> and Ni<sup>2+</sup>, respectively. The adsorption of the two metallic ions was carried out on diatomite and palygorskite under the same conditions. The thermodynamic parameters were established by studying the adsorption of the two metallic ions, varying the temperature from 25 °C to 45 °C. The adsorption capacity at the equilibrium was calculated using Equation (1):

$$Q_t = (C_o - C_t) \times \frac{V}{m} \quad (1)$$

where

C<sub>o</sub>: the initial concentration (mg/g)

C<sub>t</sub>: the concentration at time t (mg/g)

m: the mass of adsorbent (mg)

V: the volume of solution (mL)

### 2.4. Analysis

The raw and purified diatomite was analyzed by powder XRD via a PANalytical CubiX<sup>3</sup> diffractometer using CuKα (λCuKα-media = 1.5418 Å, λCuKα1 = 1.54060 Å, λCuKα2 = 1.54439 Å) radiation (operating at 40 kV and 40 mA) over the angular range of 5–70° 2θ (step size = 0.04 and time per step = 353 s) at room temperature.

The chemical composition of the diatomite sample (before and after the treatment) was measured by XRF technique using PANalytical AXIOS (WDXRF) spectrometer (Almelo, the Netherlands).

Diatomite and palygorskite were characterized by attenuated total reflectance, FTIR spectroscopy (ATR-FTIR, PerkinElmer Spectrum, London, UK) in the range from 450 to 4000 cm<sup>−1</sup> with a resolution of 8 cm<sup>−1</sup>. Diatomite and palygorskite were characterized by attenuated total reflectance, FTIR spectroscopy (ATR-FTIR, PerkinElmer Spectrum) in the range from 450 to 4000 cm<sup>−1</sup> with a resolution of 8 cm<sup>−1</sup>.

### 3. Results and Discussions

#### 3.1. Characterization of Adsorbents

##### 3.1.1. XRF Studies

The chemical composition of the samples was obtained by X-ray fluorescence (XRF) technique (Almelo, the Netherlands). Table 1 shows that the raw material contains low quantities of SiO<sub>2</sub> (29.60%) with small quantities of other minerals components. However, the amount of silica increased to 78.83% after using HCl solution. These results of XRF analysis are in agreement with those reported by Li and coauthors, although the diatomite was from different sources containing mainly SiO<sub>2</sub> with percentage ranging from 62.8 to 90.1% [20].

In general, the quantities of SiO<sub>2</sub> on palygorskite do not exceed 60% [21]. As shown in Table 1, after the modification, the amount of SiO<sub>2</sub> decreased to 33.5% while the quantity of mineral compounds such as MgO increased to 9.71%. Similar results were found in a previous analysis of two natural Algerian palygorskites which contained 39.314 and 7.930% of SiO<sub>2</sub> and MgO, respectively, for the first form of palygorskite and 40.317% (SiO<sub>2</sub>) and 8.876% (MgO) for the second form of clay [22].

**Table 1.** Composition of natural diatomite (before and after treatment) and palygorskite.

Chemical Compound	Diatomite before Treatment (%)	Diatomite after Treatment (%)	Palygorskite(%)
SiO <sub>2</sub>	29.60	78.83	33.65
Al <sub>2</sub> O <sub>3</sub>	2.57	6.53	3.16
Fe <sub>2</sub> O <sub>3</sub>	1.08	2.52	9.71
MnO	0.00	0.00	0.01
MgO	5.78	2.01	9.92
CaO	0.20	0.59	5.35
Na <sub>2</sub> O	26.89	0.00	4.12
K <sub>2</sub> O	0.39	0.96	0.47
TiO <sub>2</sub>	0.16	0.38	0.19
P <sub>2</sub> O <sub>5</sub>	4.12	0.05	1.90
LOI	28.11	8.10	29.53

LOI: Loss of ignition

##### 3.1.2. XRD Studies

Figure 1 shows the diffractogram of the 3 samples determined by X-ray diffraction. The analysis of the raw material confirmed that the latter contained small quantities of silica with different mineral components. Three mineral phases were identified: the calcite CaCO<sub>3</sub>, dolomite CaMg(CO<sub>3</sub>)<sub>2</sub> and Ca<sub>5</sub>(PO<sub>3</sub>)<sub>4</sub>(OH,F,Cl) in the region 20–25°2θ. Thus, this sample corresponds to a diatomite that is not pure, however, it contains large amounts of other minerals according to the existence of different kinds of clay minerals (palygorskite, sepiolite and smectites).

As shown in Figure 1a, the characteristic peaks of treated diatomite were 21.76, 26.66 and 31.96. Thus three crystalline polymorphs of silica were identified as SiO<sub>2</sub> (cristobalite, tridymite and quartz) and the sample contained significant amounts of amorphous (noncrystalline) material and kept the quantities of mineral clays after treatment (the small peaks at low values of 2θ). Then, the acid solution has eliminated carbonates, calcite and dolomite, as well as apatite; however, it did not remove clays such as palygorskite [23].

Figure 1b shows the new sample was a complex mixture of amorphous material with a set of minerals: The SiO<sub>2</sub> still existed under its three allotropic forms. The typical diffraction peak in 2θ = 8.57 can confirm the presence of the palygorskite plane crystal face [24]. The peaks in 2θ = 21.93, 29.58 and 32.20 indicate a monoclinic symmetry with C<sub>2</sub>/m space group [25]. The diffractograms confirmed that the palygorskite type Mg<sub>5</sub>(Si,Al)<sub>8</sub>O<sub>20</sub>(OH)<sub>2</sub>·8H<sub>2</sub>O was formed successfully from the modified diatomite.

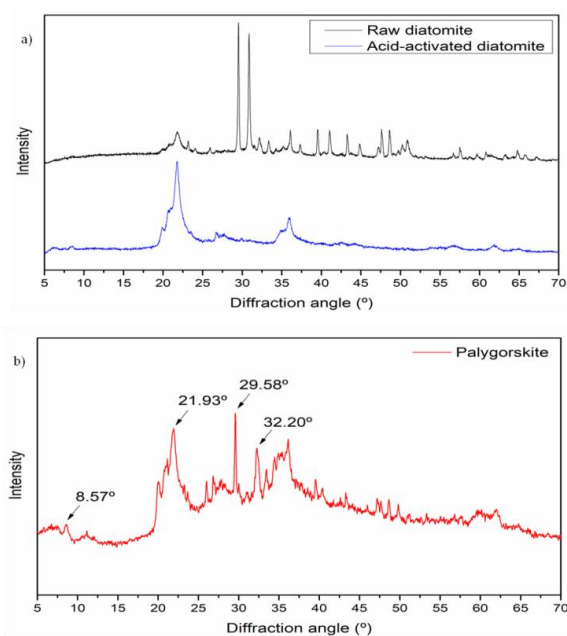


**Figure 1.** Analyses of XRD for (a) raw and purified diatomite; (b) palygorskite.

### 3.1.3. FTIR studies

FTIR (Fourier-transform infrared spectroscopy) was carried out between  $450$  and  $4000\text{ cm}^{-1}$  to analyze the surface characteristics of diatomite (before and after treatment) and palygorskite (Figure 2). The peak at  $876$  and  $1431\text{ cm}^{-1}$  confirmed the presence of calcite in the raw diatomite. As shown in Figure 2, two absorption peaks at  $3328\text{ cm}^{-1}$  and  $1658\text{ cm}^{-1}$  were related to the O–H vibration of the physically absorbed  $\text{H}_2\text{O}$  and structural hydroxyl groups were recorded [26]. The other two vibrations at around  $1023\text{ cm}^{-1}$  and  $465\text{ cm}^{-1}$  were related to the asymmetric stretching vibration mode of siloxane (Si–O–Si) [27]. The peak at  $786\text{ cm}^{-1}$  was attributed to Al–O–Si stretching vibration according to the clay minerals in diatomite [28].

The most changes resulting after treatment was the disappearance of the two bands at  $875$  and  $1431\text{ cm}^{-1}$ .

The strong band around band at  $3395\text{ cm}^{-1}$  was attributed to the hydroxide stretching of Mg/Fe–OH [29] of the surface of the sample. In addition, the appearance of two peaks at  $1642$  and  $1480\text{ cm}^{-1}$  confirms the coordination with Mg. Furthermore, the band at  $1029\text{ cm}^{-1}$  corresponds to the Si–O–Si stretching and the peak at  $1329\text{ cm}^{-1}$  corresponds to the stretching vibration of Al–O–Si.

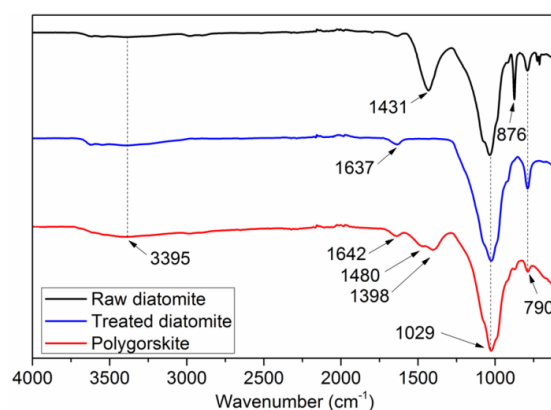


**Figure 2.** FTIR spectra of raw and treated diatomite and palygorskite.

### 3.2. Adsorption Kinetics

#### 3.2.1. Effect of Contact Time and Initial Concentration of the Adsorption of Copper and Nickel by Treated Diatomite and Palygorskite

The contact time is an important factor affecting the adsorption process. The experiment was carried out in 50 mL of solution with 0.5 g of adsorbents at 25 °C. The effect of contact time on copper and nickel removal by the two samples is shown in Figure 3. It is clear that the removal efficiency of 100 mg/L of  $\text{Cu}^{2+}$  solution was a rapid process and reached 73% and 85.44% on diatomite and palygorskite, respectively, within the first 20 min. In addition, an increase of the contact time favored the increase of  $\text{Cu}^{2+}$  removal to 78.44% on diatomite and 91% on palygorskite when the adsorption process reached equilibrium after 90 min. The adsorption process of  $\text{Ni}^{2+}$  occurred in two different phases: fast phase from 0 to 20 min and slow phase after 20 min. The removal capacity of diatomite was 67.96% before 20 min and increased to 77.3%; however, the (%) of adsorption capacity was, in the first phase, 79.58% on palygorskite and increased in the second phase to 89.97%. This fact is due to the decrease of the available sites due to the saturation of the adsorbent surface by the metal. Moreover, Figure 4 shows that the (%) of the removal of metallic ions was strongly dependent on the initial concentration of  $\text{Cu}^{2+}$  and  $\text{Ni}^{2+}$  ions. The effect of initial metal concentration on the (%) of the adsorption process was carried at room temperature and the initial pH chosen was 4 for  $\text{Cu}^{2+}$  and 7 for  $\text{Ni}^{2+}$ . The results indicate that the adsorption capacity of diatomite and palygorskite increased positively with the initial concentration of the metal ion. Thus, this increase is due to the presence of the driving force of concentration allowing an increase of the residence between the adsorbent and solution [30]. As observed in a previous study, the adsorption of  $\text{Cu}^{2+}$  on three materials (chitin (CH), chitosan (CS) and chitosan-ethylenediaminetetra-acetic acid (CS-EDTA)) occurs in two steps: rapid step from 0 to 30 min and slow step after 30 min. The adsorption capacity of CS-EDTA was 110 mg/L, Cs 67 mg/L and CH 58 mg/L for the same concentration of  $\text{Cu}^{2+}$  (300 mg/L) [31]. In other work, the effect of contact time on the removal of 20 mg/L of  $\text{Mn}^{2+}$ ,  $\text{Fe}^{2+}$ ,  $\text{Ni}^{2+}$  and  $\text{Cu}^{2+}$  on activated carbon obtained from cow bone was studied and the removal increased with time and reached a maximum after 20 min of agitation for the four heavy metals ions [32].

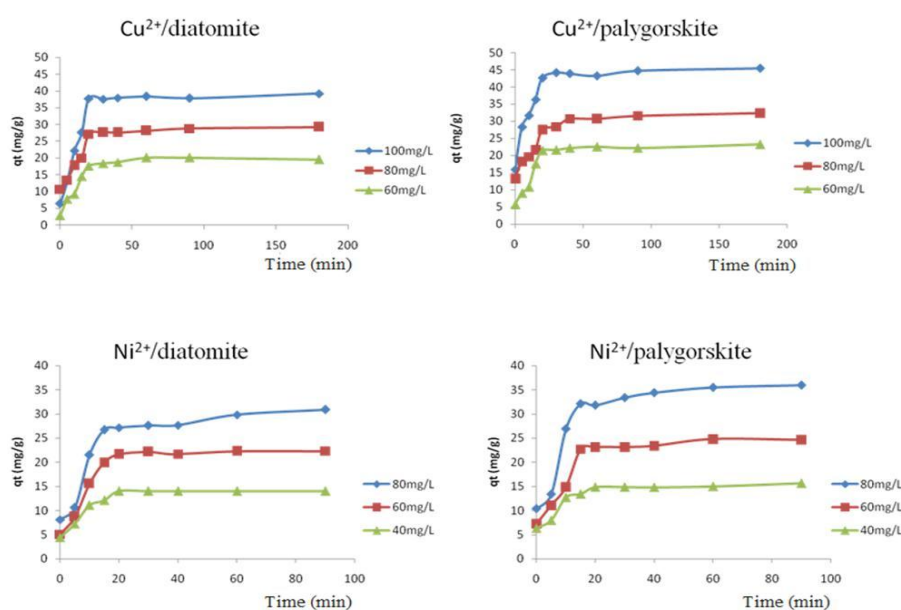


**Figure 3.** Effect of contact time on the adsorption of Cu(II) and Ni(II) on diatomite and palygorskite at different concentration ( $m_{\text{adsorbent}} = 0.5$  g,  $v = 300$  rpm,  $T = 25$  °C,  $\text{pH}_{\text{Cu}^{2+}} = 7$ ,  $\text{pH}_{\text{Ni}^{2+}} = 4$ ).

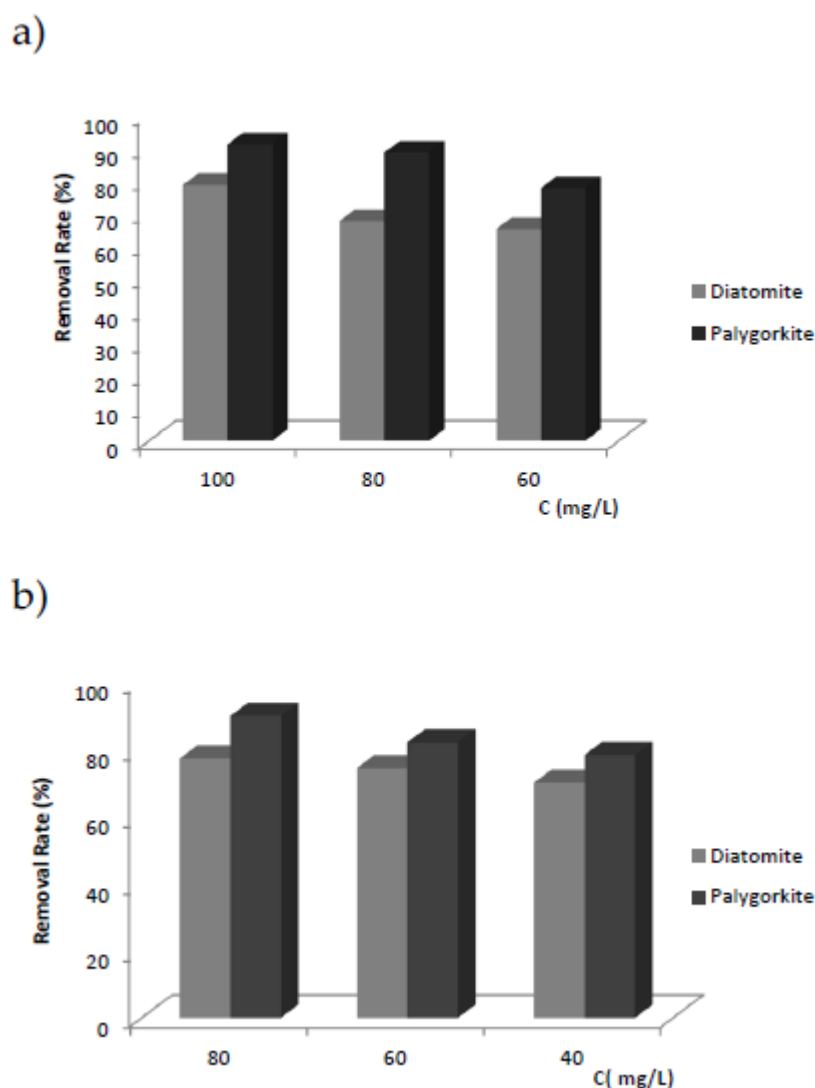


**Figure 4.** Percentage of removal of Cu<sup>2+</sup> and Ni<sup>2+</sup> by diatomite and palygorskite ( $m_{\text{adsorbent}} = 0.5 \text{ g}$ ,  $v = 300 \text{ rpm}$ ,  $T = 25 \text{ }^\circ\text{C}$ ,  $\text{pH}_{\text{Cu}^{2+}} = 4$ ,  $\text{pH}_{\text{Ni}^{2+}} = 7$ ).

### 3.2.2. Comparative Experiment

To avoid the precipitation of the metal ions at pH 6 for Cu<sup>2+</sup> and 8 for Ni<sup>2+</sup> and to compare the capacity adsorption of diatomite and clay, the initial solution pH was adjusted at 4 (Cu<sup>2+</sup>) and 7 (Ni<sup>2+</sup>). The maximum adsorption capacities of diatomite were 38.093 mg/g (Cu<sup>2+</sup>) and 28.65 mg/g (Ni<sup>2+</sup>) and increased, in the same condition, to 44.06 mg/g (Cu<sup>2+</sup>) and 34.23 mg/g for (Ni<sup>2+</sup>) for palygorskite. The results indicate that palygorskite is the most efficient. The comparison between our results and adsorption capacities of materials reported in the literature is important despite the difficulties related to the difference in experimental conditions. For example, in previous work, it was demonstrated that zeolite and clay are more efficient than diatomite for the removal of Cu<sup>2+</sup> with adsorption capacities 0.128, 0.096 and 0.047 mmol/g at pH 5 for zeolite, clay and diatomite, respectively [33]. In other work, the adsorption of Cu<sup>2+</sup> and Ni<sup>2+</sup> was studied on two different adsorbents (palygorskite and vermiculite); the maximum adsorption on palygorskite was 12.53 mg/g (Cu<sup>2+</sup> at pH 5.10) and 11.57 mg/g (Ni<sup>2+</sup> at pH 4.85), however, the maximum adsorption increased using the vermiculite as adsorbent (32.68 mg/g for Cu<sup>2+</sup> and 37.85 mg/g for Ni<sup>2+</sup>) [34].

### 3.2.3. Effect of pH

The pH value of the aqueous solution is a significant parameter in the adsorption process. Thus, the dependence of the adsorption process on pH is due to the consumption of the metallic ion as metal hydroxide ion pairs or precipitates and the competition between the hydrogen ions and the metal for the active sites on the surface. Moreover, the mechanism of adsorption at the surface of the adsorbent can reflect the nature of physicochemical interactions between the metal ions and the active sites of diatomite or palygorskite in the solution. In order to determine the effect of pH, the experiments were performed at different initial pHs ranging from 2 to 11. The analysis of the results, presented in Figure 5, shows that the adsorption capacity of the two materials reached a maximum at pH = 7 for Ni<sup>2+</sup> and at pH = 5 for Cu<sup>2+</sup>. The experiments show that the optimum pH was 6 for Ni<sup>2+</sup> and 4 for Cu<sup>2+</sup>, since the copper ions precipitate as hydroxide Cu(OH)<sub>2</sub> at pH > 4 and the nickel ions precipitate as hydroxide Ni(OH)<sub>2</sub> at pH > 7. Thus, the precipitation of copper hydroxide and nickel hydroxide caused a decrease of the adsorption capacity and their removal from solution at these pHs is not due to the adsorption process. Comparing to previous work of the adsorption of Ni<sup>2+</sup> and Cu<sup>2+</sup> by  $\gamma$ -alumina nanoparticles, the optimum pH was 6 for Ni<sup>2+</sup> and 5 for Cu<sup>2+</sup> and it was demonstrated that the adsorption capacity increased with the pH, which is not due to the adsorption process [35]. In other work about the adsorption of heavy metals on natural iron-oxide-coated sand, it was demonstrated that the optimum pH was 7 for Ni<sup>2+</sup> and 5 for Cu<sup>2+</sup>; the effects of pH changes were explained by the type of the adsorbent, its behavior in the solution and the type of adsorbed ions [36].

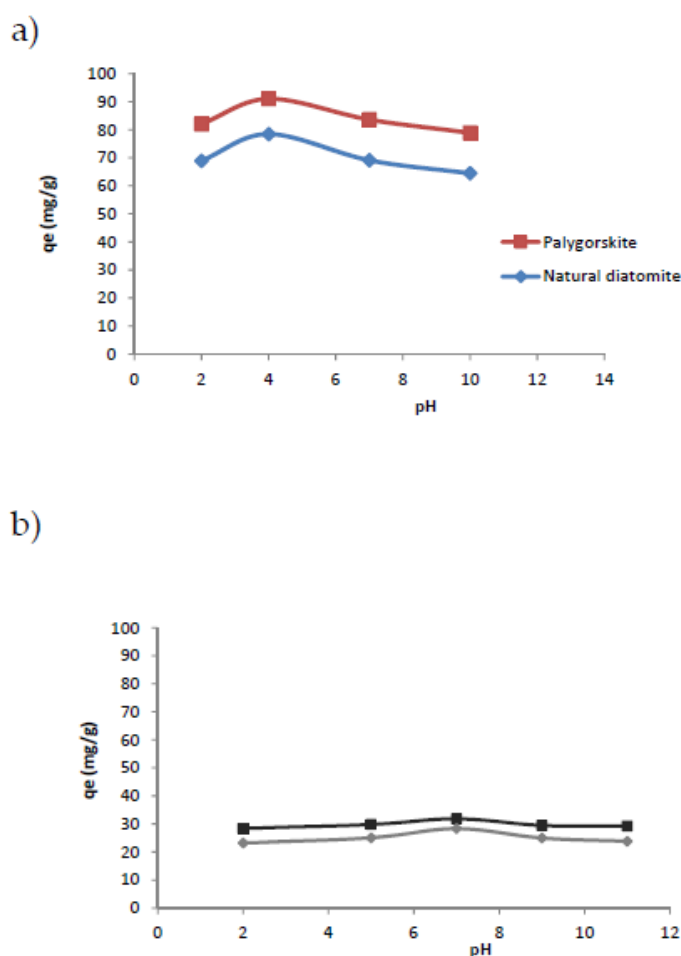


**Figure 5.** Effect of pH on the adsorption of Cu<sup>2+</sup> (a) and Ni<sup>2+</sup> (b) on diatomite and palygorskite ( $m_{\text{adsorbent}} = 0.5$  g,  $v = 300$  rpm).



### 3.2.4. Effect of Temperature

Several previous studies have investigated the effect of temperature on heavy metal uptake. In this study, the removal of  $\text{Cu}^{2+}$  and  $\text{Ni}^{2+}$  from aqueous solution using diatomite and palygorskite has been investigated at three different temperatures ranging from 25 to 45 °C. As noted, the  $\text{Cu}^{2+}$  and  $\text{Ni}^{2+}$  adsorption decreased as the temperature increased. This decrease with temperature can be due to the weakening of attractive forces between metal ions and adsorbent.

### 3.2.5. Stimulation Modeling of Adsorption Data

In the present study, the pseudo-first-order kinetic and pseudo-second-order kinetic were used for the interpretation of the kinetic batch experiment. The equation of the pseudo-first-order model proposed by Lagergren [37] can be written as follows:

$$\log(q_e - q_t) = -k_1 t \log q_e \quad (2)$$

where:

$q_t$ : the amount of solute adsorption at different time

$k_1$ : the constant of pseudo-first-order model

$q_e$ : the equilibrium adsorption capacity

The equation of the pseudo-second-order model equation as given by Ho and McKay [38] can be expressed as:

$$\frac{t}{q_t} = \frac{1}{k_2 \cdot q_e^2} \frac{1}{q_e} \times t \quad (3)$$

where:

$q_t$ : the amount of solute adsorption at different time

$q_e$ : the equilibrium adsorption capacity

$k_2$  (g/mg min): the rate constant of pseudo-second-order adsorption

The results reported in Table 2 show that the coefficient of correlation ( $R^2$ ) of the pseudo-second-order model is close with 1 and the values of  $q_e$  calculated agreed with the value of  $q_e$  experimental. However, the results of the pseudo-first-order model are completely different with coefficient of correlation far then the unity and the two values of  $q_e$  calculated and  $q_e$  experimental are different. These values evidence that the pseudo-second-order model is valid to describe the kinetic adsorption of  $\text{Cu}^{2+}$  and  $\text{Ni}^{2+}$  on diatomite and palygorskite [39].

**Table 2.** Parameters for kinetics models for  $\text{Cu}^{2+}$  and  $\text{Ni}^{2+}$  adsorption onto treated diatomite.

Adsorbents	Kinetic Models	Parameters	$\text{Ni}^{2+}$				$\text{Cu}^{2+}$	
			80 mg/L	60 mg/L	40 mg/L	100 mg/L	80 mg/L	60 mg/L
Natural diatomite	Pseudo-first-order	$q_{ecal}$ (mg/g)	15.35	13.93	4.27	11.18	21.23	18.75
		$q_{eexp}$ (mg/g)	28.65	22.02	14.02	38.09	28.08	19.06
		$K_1$ ( $\text{min}^{-1}$ )	0.036	0.047	0.049	0.025	0.046	0.047
		$R^2$	0.815	0.796	0.765	0.553	0.869	0.965
	Pseudo-second-order	$q_{ecal}$ (mg/g)	32.25	23.81	14.49	41.67	30.3	20.41
		$q_{eexp}$ (mg/g)	30.91	22.02	14.02	38.09	28.08	19.06
		$K_2$ (g/mg.min)	0.0067	0.013	0.034	0.0051	0.0081	0.0108
		$R^2$	0.991	0.993	0.997	0.996	0.996	0.995
Palygorskite	Pseudo-first-order	$q_{ecal}$ (mg/g)	24.77	13.39	6.92	17.46	19.055	9.42
		$q_{eexp}$ (mg/g)	34.231	23.83	15.04	44.07	30.17	22.2
		$K_1$ ( $\text{min}^{-1}$ )	0.052	0.0743	0.047	0.032	0.034	0.0343
		$R^2$	0.925	0.811	0.803	0.68	0.907	0.753
	Pseudo-second-order	$q_{ecal}$ (mg/g)	38.46	26.32	16.13	47.62	33.33	24.39
		$q_{eexp}$ (mg/g)	34.231	23.83	15.04	44.07	30.17	22.2
		$K_2$ (g/mg.min)	0.0068	0.0103	0.027	0.081	0.00671	0.00804
		$R^2$	0.993	0.993	0.997	0.999	0.998	0.996

### 3.3. Adsorption Isotherms

In our work, Langmuir and Freundlich models were checked to quantify the adsorption capacity of diatomite and palygorskite.

#### 3.3.1. Langmuir Isotherm

The Langmuir model is an indication of a monolayer adsorption onto homogeneity of the surface of adsorbents with identical sites. It can be expressed by the equation as follows:

$$\frac{1}{q_e} = \left( \frac{1}{q_m} \right) + (1/(K_L \times C_e \times q_m)) \quad (4)$$

where

$q_e$ : quantity adsorbed at equilibrium

$C_e$ : the concentration of metals adsorbed at equilibrium

$q_m$ : constant related to the area occupied by a monolayer of adsorbate reflecting the adsorption capacity (mg/g)

$K_L$ : Langmuir constant

#### 3.3.2. Freundlich Isotherm

The Freundlich model is available for a multilayer gas adsorption onto heterogeneity of the surface of adsorbents without uniform distribution of adsorption energy and affinities.

The Freundlich equation model is given as follows:

$$\log q_e = \log K_f + \frac{1}{n} \log C_e \quad (5)$$

where:

$q_e$ : quantity adsorbed at equilibrium

$C_e$ : concentration at equilibrium

$K_f$ : Freundlich constant

The values calculated from those two models are listed in Table 3. The adsorption of copper and nickel was well represented by the Langmuir isotherm with a coefficient of correlation close to 1. As shown in Table 3, the value of maximum adsorption capacity on diatomite  $q_m$  calculated was 111.10 mg/g and 90.91 mg/g for  $Cu^{2+}$  and  $Ni^{2+}$ , respectively and on palygorskite, it was 333.33 mg/g for  $Cu^{2+}$  and 166.67 mg/g for  $Ni^{2+}$ . Those values are higher than  $q_m$  calculated in a previous study [40] where the maximum adsorption capacity of copper on acid-activated palygorskite was 93.02 mg/g. Petra et al. found  $q_m$  295 mg/g for the adsorption of  $Cu^{2+}$  on activated saponite and 129 mg/g for  $Ni^{2+}$  on the same adsorbent [41]. In addition, Igherese and coworkers [42] demonstrated that the maximum adsorption capacity of  $Cu^{2+}$  on polyaniline-grafted chitosan was 83.30 mg/g. Senthil Kumar [43] reported a maximum adsorption capacity of cashew nutshell of 18.868 mg/g. Furthermore, the  $q_m$  of the barley straw for the biosorption of nickel was 35.8 mg/g [44]. The biosorption of nickel using waste pomace from an olive oil factory was also low based on the value  $q_m$ , which was 14.8 mg/g [45]. Compared with these adsorbents, it is clear that palygorskite prepared from diatomite has a good adsorption capacity. The high value of  $q_m$  can be due to the homogeneous distribution of high-energy sites on the surface of the adsorbents. As given in Table 3, the value of  $K_L$  (diatomite) was higher than  $K_L$  of palygorskite, indicating the lower affinities of the surface of diatomite than the surface of palygorskite. The value of  $n$ , calculated from the Freundlich equation, is superior than 1 indicates that the adsorption is favorable and the high values of  $K_f$  indicate a very high adsorption capacity for copper and nickel adsorption in aqueous solution.

**Table 3.** Langmuir and Freundlich isotherm parameters for Cu<sup>2+</sup> and Ni<sup>2+</sup> adsorption onto treated diatomite and palygorskite.

Adsorbents	Metals ions	Parameters of Freundlich			Parameters of Langmuir		
		K <sub>f</sub>	1/n	R <sup>2</sup>	q <sub>m</sub> (mg/g)	K <sub>l</sub> (L/mg)	R <sup>2</sup>
Palygorskite	Cu <sup>2+</sup>	2.028	0.914	0.995	333.33	0.005	0.994
	Ni <sup>2+</sup>	2.87	0.848	0.994	166.67	0.014	0.992
	Cu <sup>2+</sup>	3.062	0.694	0.999	111.10	0.014	0.999
Natural Diatomite	Ni <sup>2+</sup>	2.42	0.757	0.995	90.91	0.0176	0.997

### 3.4. Thermodynamic Studies

The effect of temperature was investigated from 25 °C to 45 °C on the removal efficiency of the adsorbents using 100 mg/L of Cu<sup>2+</sup> and 80 mg/L of Ni<sup>2+</sup>. The adsorption capacities of these two adsorbents decreased with increasing temperature. The decrease of uptake of copper and nickel ions at a higher temperature indicated the exothermic adsorption. The thermodynamic parameters, such as ΔG°, ΔH° and ΔS°, were determined to evaluate the effect of temperature, using the following equations:

$$K_c = \frac{C_a}{C_e} \quad (6)$$

$$\Delta G^\circ = -RT \ln K_c \quad (7)$$

$$\ln K_c = \frac{\Delta S^\circ}{R} - \frac{\Delta H^\circ}{RT} \quad (8)$$

$$\Delta G^\circ = \Delta H^\circ - T\Delta S^\circ \quad (9)$$

where:

K<sub>c</sub>: the equilibrium constant

C<sub>ads</sub>: the adsorbent phase concentration at equilibrium (mg/L)

C<sub>e</sub>: the equilibrium concentration in solution (mg/L)

R: the universal gas constant (KJ/mol K)

T: the solution temperature (K)

The thermodynamic parameters are shown in Table 4. The values of ΔH° (KJ·mol<sup>-1</sup>) and ΔS° (KJ·mol<sup>-1</sup>) were obtained from the slope and intercept of a plot of lnK<sub>d</sub> versus 1/T. In general, the change of free energy for the physisorption is in the interval (−80–0) KJ·mol<sup>-1</sup> and the chemisorption is in the interval (−400–80) KJ·mol<sup>-1</sup>. In our study, the values of ΔH° are in the interval (−80–0) KJ·mol<sup>-1</sup>, indicating a physical adsorption process. It can be seen from Table 4 that ΔH° values are negative, thus the distribution coefficient values K<sub>d</sub> increased with the increase of temperature, which shows the exothermic nature of the adsorption involving low “van der Waals” attraction forces type and confirms the decrease of the adsorption capacity of metal when the temperature increases [46]. In addition, the values of ΔS° were negative, corresponding to a decrease in the degree of freedom of adsorbed species and shows the decrease in the randomness at the solid-solution interface of Cu<sup>2+</sup> and Ni<sup>2+</sup> onto the palygorskite and diatomite surface, which would cause a decrease in entropy during the adsorption process. Furthermore, the values of ΔS° for the adsorption of Ni<sup>2+</sup> onto palygorskite and diatomite for the two metals ions from 25 °C to 45 °C are negative, indicating a spontaneous and favorite adsorption process. However, the values of ΔG° are positive at 35 and 45 °C for the adsorption of Cu<sup>2+</sup>, indicating that the adsorption was not favorite and not spontaneous [47].

**Table 4.** Thermodynamic parameters for the adsorption of Cu<sup>2+</sup> and Ni<sup>2+</sup> onto treated diatomite and palygorskite.

Materials	Metals Ions	T (°C)	$\Delta^{\circ}H(KJ\cdot mol^{-1})$	$\Delta^{\circ}S(KJ\cdot mol^{-1})$	$\Delta^{\circ}G(KJ\cdot mol^{-1})$
	Cu <sup>2+</sup>	25	−23.15	−0.069	−2.46
		35			−1.93
		45			−1.07
Palygorskite	Ni <sup>2+</sup>	25	−17.70	−0.46	−4.10
		35			−3.71
		45			−9.19
Diatomite	Cu <sup>2+</sup>	25	−22.34	−0.07	−0.56
		35			0.51
		45			0.85
	Ni <sup>2+</sup>	25	−13.64	−0.069	−2.72
		35			−2.17
		45			−1.99

#### 4. Conclusions

In this study, diatomaceous earth was used to prepare palygorskite clay. The characterization of modified diatomite confirms that palygorskite was prepared successfully. These two mineral adsorbents were used for copper and nickel removal in aqueous solution and compared. The results and the parameters obtained indicated that palygorskite clay is able to remove Cu<sup>2+</sup> and Ni<sup>2+</sup> ions. Moreover, the removal of metal ions increases using palygorskite as an adsorbent. Palygorskite showed better results than natural diatomite. Furthermore, the results obtained from different initial concentrations of Cu(II) and Ni(II) show that Freundlich and Langmuir isotherms can be used to fit the data and estimate model parameter. The adsorption kinetics of metals ions onto diatomite and palygorskite can be described by the pseudo-second-order model. The values of thermodynamic parameters showed that the adsorption of Cu<sup>2+</sup> and Ni<sup>2+</sup> was spontaneous and exothermic. According to the results of the pH effect, the maximum adsorption was detected at pH 4 for Cu<sup>2+</sup> (II) and pH 7 for Ni<sup>2+</sup>. The decrease of the adsorption capacity at higher values of pH is due to the precipitation of copper hydroxide Cu (OH)<sub>2</sub> and nickel hydroxide Ni(OH)<sub>2</sub>. The results of the present work confirmed that palygorskite prepared from Tunisian diatomite has a good and important potential to be used as an efficient adsorbent to remove heavy metals from effluents.

**Author Contributions:** Conceptualization, J.L. and H.N.; Methodology, M.A. and S.A.; Investigation, H.N.; Writing-Original Draft Preparation, H.N.; Writing-Review & Editing, J.L. and S.A.; Funding Acquisition, J.L.

**Funding:** This research was funded by Department of Education of the Basque Government grant number [IT1008-16]” and “The APC was funded by Department of Education of the Basque Government.

**Acknowledgments:** This research was financially supported by the Department of Education of Basque Government (IT1008-16).

**Conflicts of Interest:** The authors declare no conflict of interest.

#### References

- Barros, F.C.; Sousa, F.W.; Cavalcante, R.M.; Carvalho, T.V.; Dias, F.S.; Queiroz, D.C.; Nascimento, R.F. Removal of Copper, Nickel and Zinc Ions from Aqueous Solution by Chitosan-8-Hydroxyquinoline Beads. *CLEAN—Soil Air Water* **2008**, *36*, 292–298. [[CrossRef](#)]
- Revathi, M.; Ahmed Basha, C.; Velan, M. Removal of copper (II) ions from synthetic electroplating rinse water using polyethyleneimine modified ion-exchange resin. *Desalin. Water. Treat.* **2016**, *57*, 20350–20367. [[CrossRef](#)]
- Aliabadi, M.; Irani, M.; Ismaeili, J.; Najafzadeh, S. Design and evaluation of chitosan/hydroxyapatite composite nanofiber membrane for the removal of heavy metal ions from aqueous solution. *J. Taiwan Inst. Chem.* **2014**, *45*, 518–526. [[CrossRef](#)]

4. Zhu, Y.; Chen, T.; Liu, H.; Xu, B.; Xie, J. Kinetics and thermodynamics of Eu (III) and U (VI) adsorption onto palygorskite. *J. Mol. Liq.* **2016**, *219*, 272–278. [[CrossRef](#)]
5. Yariv, S.; Borisover, M.; Lapides, I. Few introducing comments on the thermal analysis of organoclays. *J. Therm. Anal. Calorim.* **2011**, *105*, 897–906. [[CrossRef](#)]
6. Gionis, V.; Kacandes, G.H.; Kastritis, I.D.; Chryssikos, G.D. Combined near-infrared and X-ray diffraction investigation of the octahedral sheet composition of palygorskite. *Clays Clay Miner.* **2007**, *55*, 543–553. [[CrossRef](#)]
7. Fois, E.; Gamba, A.; Tilocca, A. On the unusual stability of Maya blue paint: molecular dynamics simulations. *Microporous Mesoporous Mater.* **2003**, *57*, 263–272. [[CrossRef](#)]
8. Zhang, Y.; Wang, W.; Zhang, J.; Liu, P.; Wang, A. A comparative study about adsorption of natural palygorskite for methylene blue. *Chem. Eng. J.* **2015**, *262*, 390–398. [[CrossRef](#)]
9. Khademi, H.; Arocena, J.M. Kaolinite formation from palygorskite and sepiolite in rhizosphere soils. *Clays Clay Miner.* **2008**, *56*, 429–436. [[CrossRef](#)]
10. Chaisena, A.; Rangriwatananon, K. Synthesis of sodium zeolites from natural and modified diatomite. *Mater. Lett.* **2005**, *59*, 1474–1479. [[CrossRef](#)]
11. Tsai, W.T.; Lai, C.W.; Hsien, K.J. Characterization and adsorption properties of diatomaceous earth modified by hydrofluoric acid etching. *J. Colloid Interface Sci.* **2006**, *297*, 749–754. [[CrossRef](#)] [[PubMed](#)]
12. Pantoja, M.L.; Jones, H.; Garelick, H.; Mohamedbakr, H.G.; Burkitbayev, M. The removal of arsenate from water using iron-modified diatomite (D-Fe): isotherm and column experiments. *Environ. Sci. Pollut. Res.* **2014**, *21*, 495–506. [[CrossRef](#)] [[PubMed](#)]
13. Xia, P.; Wang, X.; Wang, X.; Zhang, J.; Wang, H.; Song, J.; Zhao, J. Synthesis and Characterization of MgO Modified Diatomite for Phosphorus Recovery in Eutrophic Water. *J. Chem. Eng. Data.* **2016**, *62*, 226–235. [[CrossRef](#)]
14. He, X.; Yang, Q.; Fu, L.; Yang, H. Synthesis and magnetic property of SiO<sub>2</sub> coated Fe<sub>3</sub>O<sub>4</sub>/palygorskite. *Funct. Mater. Lett.* **2015**, *8*, 56–155. [[CrossRef](#)]
15. Lai, S.; Yue, L.; Zhao, X.; Gao, L. Preparation of silica powder with high whiteness from palygorskite. *Appl. Clay Sci.* **2010**, *50*, 432–437. [[CrossRef](#)]
16. Korus, I.; Rumińska, M. UV spectrophotometric studies of Cu (II) ions separation by ultrafiltration enhanced with poly (sodium acrylate). *Desalin. Water* **2016**, *57*, 1436–1442. [[CrossRef](#)]
17. Bermejo-Barrera, A.; Bermejo-Barrera, P.; Martinez, F.B. Simultaneous determination of copper and cobalt with EDTA using derivative spectrophotometry. *Analyst* **1985**, *110*, 1313–1315. [[CrossRef](#)]
18. Zhang, X.; Wang, X. Adsorption and desorption of nickel (II) ions from aqueous solution by a lignocellulose/montmorillonite nanocomposite. *PLoS ONE* **2015**, *10*, e0117077. [[CrossRef](#)] [[PubMed](#)]
19. Zhang, S.; Cui, M.; Zhang, Y.; Yu, Z.; Meng, C. Synthesis of zeolite Y from diatomite and its modification by dimethylglyoxime for the removal of Ni (II) from aqueous solution. *J. Sol-Gel Sci. Technol.* **2016**, *80*, 215–225. [[CrossRef](#)]
20. Li, X.Y.; Jiang, Y.; Liu, X.Q.; Shi, L.Y.; Zhang, D.Y.; Sun, L.B. Direct Synthesis of Zeolites from a Natural Clay, Attapulgit. *ACS Sustain. Chem. Eng.* **2017**, *5*, 6124–6130. [[CrossRef](#)]
21. Simões, K.M.; Novo, B.L.; Felix, A.A.; Afonso, J.C.; Bertolino, L.C.; Silva, F.A. Ore Dressing and Technological Characterization of Palygorskite from Piauí/Brazil for Application as Adsorbent of Heavy Metals: In Characterization of Minerals, Metals and Materials. In *Characterization of Minerals, Metals and Materials*; Springer: Cham, Switzerland, 2017; pp. 261–267.
22. Belaroui, L.S.; Dali Youcef, L.; Ouali, A.F.F.A.F.; Bengueddach, A.B.D.E.L.K.A.D.E.R.; Lopez Galindo, A. Mineralogical and chemical characterization of palygorskite from East-Algeria. *Rev. Soc. Esp. Miner. Macla* **2014**, *19*. Available online: [http://www.ehu.eus/sem/macla\\_pdf/macla19/Belaroui.et.al\\_SEM2014.WEB.pdf](http://www.ehu.eus/sem/macla_pdf/macla19/Belaroui.et.al_SEM2014.WEB.pdf) (accessed on 14 September 2018).
23. Cai, Y.; Xue, J.; Polya, D.A. A Fourier transform infrared spectroscopic study of Mg-rich, Mg-poor and acid leached palygorskites. *Spectrochim. Acta Part A* **2007**, *66*, 282–288. [[CrossRef](#)] [[PubMed](#)]
24. Sheng, G.; Wang, S.; Hu, J.; Lu, Y.; Li, J.; Dong, Y.; Wang, X. Adsorption of Pb (II) on diatomite as affected via aqueous solution chemistry and temperature. *Coll. Surf. A* **2009**, *339*, 159–166. [[CrossRef](#)]
25. da Silva, M.L.D.G.; Fortes, A.C.; Oliveira, M.E.R.; de Freitas, R.M.; da Silva Filho, E.C.; Soares, M.F.D.L.R.; da Silva Leite, C.M. Palygorskite organophilic for dermopharmaceutical application. *J. Therm. Anal. Calorim.* **2014**, *115*, 2287–2294. [[CrossRef](#)]

26. Nourmoradi, H.; Nikaeen, M.; Khiadani, H.H. Removal of benzene, toluene, ethylbenzene and xylene (BTEX) from aqueous solutions by montmorillonite modified with nonionic surfactant: Equilibrium, kinetic and thermodynamic study. *Chem. Eng. J.* **2012**, *191*, 341–348. [[CrossRef](#)]
27. Mohammed, J.; Nasri, N.S.; Ahmad Zaini, M.A.; Hamza, U.D.; Ani, F.N. Adsorption of benzene and toluene onto KOH activated coconut shell based carbon treated with NH<sub>3</sub>. *Int. Biodeterior. Biodegrad.* **2015**, *102*, 245–255. [[CrossRef](#)]
28. Sheshdeh, R.K.; Abbaszadeh, S.; Nikou, M.R.K.; Badii, K.; Sharafi, M.S. Liquid Phase adsorption kinetics and equilibrium of toluene by novel modified-diatomite. *J. Environ. Heal. Sci. Eng.* **2014**, *12*, 148. [[CrossRef](#)] [[PubMed](#)]
29. Rusmin, R.; Sarkar, B.; Biswas, B.; Churchman, J.; Liu, Y.; Naidu, R. Structural, electrokinetic and surface properties of activated palygorskite for environmental application. *Appl. Clay Sci.* **2016**, *134*, 95–102. [[CrossRef](#)]
30. Wan, M.W.; Kan, C.C.; Rogel, B.D.; Dalida, M.L.P. Adsorption of copper (II) and lead (II) ions from aqueous solution on chitosan-coated sand. *Carbohydr. Polym.* **2010**, *80*, 891–899. [[CrossRef](#)]
31. Labidi, A.; Salaberria, A.M.; Fernandes, S.C.; Labidi, J.; Abderrabba, M. Adsorption of copper on chitin-based materials: Kinetic and thermodynamic studies. *J. Taiwan Inst. Chem.* **2016**, *65*, 10–148. [[CrossRef](#)]
32. Moreno, J.C.; Gómez, R.; Giraldo, L. Removal of Mn, Fe, Ni and Cu ions from wastewater using cow bone charcoal. *Materials* **2010**, *3*, 452–466. [[CrossRef](#)]
33. Šljivić, M.; Smičiklas, I.; Pejanović, S.; Plečaš, I. Comparative study of Cu<sup>2+</sup> adsorption on a zeolite, a clay and a diatomite from Serbia. *Appl. Clay Sci.* **2009**, *43*, 33–40. [[CrossRef](#)]
34. Bourliva, A.; Sikalidis, A.K.; Papadopoulou, L.; Betsiou, M. Removal of Cu<sup>2+</sup> and Ni<sup>2+</sup> ions from aqueous solutions by adsorption onto natural palygorskite and vermiculite. *Clay Miner.* **2018**, *53*, 1–15. [[CrossRef](#)]
35. Fouladgar, M.; Beheshti, M.; Sabzyan, H. Single and binary adsorption of nickel and copper from aqueous solutions by  $\gamma$ -alumina nanoparticles: equilibrium and kinetic modeling. *J. Mol. Liq.* **2015**, *211*, 1060–1073. [[CrossRef](#)]
36. Boujelben, N.; Bouzid, J.; Elouear, Z. Adsorption of nickel and copper onto natural iron oxide-coated sand from aqueous solutions: study in single and binary systems. *J. Hazard. Mater.* **2009**, *163*, 376–382. [[CrossRef](#)] [[PubMed](#)]
37. Labidi, A.; Saad, A.; Abderrabba, M. Copper adsorption onto starch as biopolymer: Isothermal equilibrium and kinetic studies. *J. Chem. Pharm. Res.* **2015**, *7*, 1274–1282.
38. Lagergren, S. Zurtheorie der sogenannten adsorption gelosterstoffe, KungligaSvenskaVetenskapsakademiens. *Handlingar* **1898**, *24*, 1–39.
39. Shabani, K.S.; Ardejani, F.D.; Badii, K.; Olya, M.E. Preparation and characterization of novel nano-mineral for the removal of several heavy metals from aqueous solution: Batch and continuous systems. *Arab. J. Chem.* **2017**, *10*, S3108–S3127. [[CrossRef](#)]
40. Chen, H.; Zhao, Y.; Wang, A. Removal of Cu (II) from aqueous solution by adsorption onto acid-activated palygorskite. *J. Hazard. Mater.* **2007**, *149*, 346–354. [[CrossRef](#)] [[PubMed](#)]
41. Petra, L.; Billik, P.; Melichová, Z.; Komadel, P. Mechanochemically activated saponite as materials for Cu<sup>2+</sup> and Ni<sup>2+</sup> removal from aqueous solutions. *Appl. Clay Sci.* **2017**, *143*, 22–28. [[CrossRef](#)]
42. Igberase, E.; Osifo, P.; Ofomaja, A. The adsorption of copper (II) ions by polyaniline graft chitosan beads from aqueous solution: equilibrium, kinetic and desorption studies. *J. Environ. Chem. Eng.* **2014**, *2*, 362–369. [[CrossRef](#)]
43. Kumar, P.S.; Ramalingam, S.; Kirupha, S.D.; Murugesan, A.; Vidhyadevi, T.; Sivanesan, S. Adsorption behavior of nickel (II) onto cashew nut shell: Equilibrium, thermodynamics, kinetics, mechanism and process design. *Chem. Eng. J.* **2011**, *167*, 122–131. [[CrossRef](#)]
44. Thevannan, A.; Mungroo, R.; Niu, C.H. Biosorption of nickel with barley straw. *Bioresour. Technol.* **2010**, *101*, 1776–1780. [[CrossRef](#)] [[PubMed](#)]
45. Nuhoglu, Y.; Malkoc, E. Thermodynamic and kinetic studies for environmentally friendly Ni (II) biosorption using waste pomace of olive oil factory. *Bioresour. Technol.* **2009**, *100*, 2375–2380. [[CrossRef](#)] [[PubMed](#)]

46. Azizi, S.; MahdaviShahri, M.; Mohamad, R. Green Synthesis of Zinc Oxide Nanoparticles for Enhanced Adsorption of Lead Ions from Aqueous Solutions: Equilibrium, Kinetic and Thermodynamic Studies. *Molecules* **2017**, *22*, 831. [[CrossRef](#)] [[PubMed](#)]
47. Mushtaq, M.; Bhatti, H.N.; Iqbal, M.; Noreen, S. Eriobotrya japonica seed biocomposite efficiency for copper adsorption: isotherms, kinetics, thermodynamic and desorption studies. *J. Environ. Manag.* **2016**, *176*, 21–33. [[CrossRef](#)] [[PubMed](#)]



© 2018 by the authors. Licensee MDPI, Basel, Switzerland. This article is an open access article distributed under the terms and conditions of the Creative Commons Attribution (CC BY) license (<http://creativecommons.org/licenses/by/4.0/>).